PAPER *Special Issue on Recent Progress in Information Storage Technology*

Preparation and Characterization of (0001)-Oriented Single-Crystal Co-alloy Magnetic Thin Films

Masaaki FUTAMOTO[†a)], *Regular Member*, Kouta TERAYAMA[††], *Nonmember*, Katsuaki SATO[††], *and* Yoshiyuki HIRAYAMA[†], *Regular Members*

SUMMARY The effect of a nonmagnetic *hcp*-underlayer on the epitaxial growth of $CoCr_{19}Pt_{10}$ magnetic layers on substrates of $Al_2O_3(0001)$ single-crystal has been investigated. Thin films of (0001)-oriented single-crystal $CoCr_{19}Pt_{10}$ were obtained by employing non-magnetic underlayers of $CoCr_{25}Ru_{25}$ and $CoCr_{25}Ru_{25}/Ti$, while thin films of polycrystalline $CoCr_{19}Pt_{10}$ were grown after the deposition of underlayers of $TiCr_{10}$ and $CoCr_{40}$. The growth of thin film $CoCr_{19}Pt_{10}$ on a Ti(0001) underlayer was interpreted as quasi-hetero-epitaxial where the continuity of the lattice across the interface is disturbed while the overall crystallographic relationship between the two layers is maintained. A thin film of epitaxially grown $CoCr_{19}Pt_{10}$ has a compositional variation of a few percent across the film plane in terms of elements that forms the alloy.

key words: *Co-alloy magnetic thin films, epitaxial growth, underlayer, single-crystal substrate*

1. Introduction

Co-based alloy thin films are widely used as the magnetic recording media of hard disk drives. The areal density and data transfer rate will increase to 100–200 Gb/in^2 and 500–1000 Mb/s, respectively, within the next few years. The thermal stability of recorded information and magnetic switching speed under such ultra-high density magnetic recording have been investigated through computer simulation. Accurate values for the magnetic properties of the Co-based alloys such as its uniaxial magneto-crystalline anisotropy constant and Gilbert's damping constant are essential for such an investigation. However, it has not been easy to determine these values for thin films of polycrystalline magnetic materials which consist of very small crystalline grains and have a complicated microstructure [1].

To obtain accurate results for the basic magnetic properties, it is necessary to use well-defined thin films of the material, preferably in its single-crystal forms [2]. Thin films of single-crystal have been prepared by hetero-epitaxial growth on single-crystal substrates. Thin films of Co and Co-alloy materials with $(11\bar{2}0)$, $(10\bar{1}1)$, $(10\bar{1}0)$, and (0001) orientations have been epitaxially grown on various single-crystal substrates; the works are summarized in Table 1. Note that almost all of these films were actually grown employing some underlayer. Misfit dislocations, stacking faults, and even subgrain boundaries are generally recognizable in these thin films. These crystallographic defects are introduced to accommodate the lattice mismatch between the different materials. The crystallographic quality of an epitaxially grown thin film depends on the materials selected for the substrate and underlayer.

The effect of the substrate on the epitaxial growth of thin films of (0001)-oriented CoCrPt magnetic layer has been investigated for $Al_2O_3(0001)$, $LaAlO_3(0001)$, $SrTiO_3(111)$, and MgO(111) single-crystal substrates. In each case, a nonmagnetic underlayer was employed under similar experimental conditions [16]. The best single-crystal thin film in this work was obtained on the Al_2O_3 substrate according to this crystallographic relationship: CoCrPt(0001)[21.0] // Al_2O_3(0001)[10.0].

In this study, we focus on the effect of the underlayer on the crystallographic quality of thin films of $CoCr_{19}Pt_{10}$ grown on substrates of single-crystal $Al_2O_3(0001)$. Nonmagnetic underlayers that have been widely used as underlayers or intermediate layers in the preparation of strongly c-axis oriented CoCr-alloy perpendicular magnetic recording media [17]–[20] are employed in the epitaxial growth of the magnetic thin films. X-ray diffraction and high-resolution transmission electron microscopy (TEM) were applied to obtain structural information. The conditions under which we obtained good magnetic thin films are discussed on this basis.

2. Preparing and Characterizing the Samples

A DC sputtering system with a base pressure below 1×10^{-9} torr [17] was used to prepare the thin films. The cross-sectional structure of the sample is shown in Fig. 1(a). Figure 1(b) shows the relationship between the crystallographic orientation of a *hcp*-material and the $Al_2O_3(0001)$ substrate on which it has been epitaxially grown. The *a*-axis of the *hcp*-material is rotated by 30 degrees with respect to the *a*-axis of Al_2O_3. In our experiments, a nonmagnetic *hcp*-underlayer and a $CoCr_{19}Pt_{10}$ magnetic layer were sequentially sputter-deposited on an $Al_2O_3(0001)$ substrate which was kept at 260°C. The underlayer material with *hcp*-crystal

Manuscript received February 14, 2002.
Manuscript revised April 26, 2002.

[†]The authors are with Central Research Laboratory, Hitachi Ltd., Kokubunji-shi, 185-8601 Japan.
[††]The authors are with Tokyo University of Agriculture and Technology, Koganei-shi, 184-8588 Japan.
a) E-mail: futamoto@crl.hitachi.co.jp

Table 1 The epitaxial growth of Co and Co-alloy thin films on single-crystal substrates.

Film orientation	Underlayer	Substrate	Reference
Co(11$\bar{2}$0)	Cr(001)	NaCl(001)	Daval et al., 1970 [3]
Co-alloy(11$\bar{2}$0)	-	Cr(001)	Wong et al., 1991 [4]
Co(1120)	Cr(001)	MgO(001), LiF(001)	Nakamura et al., 1994 [5], 1995 [6]
Co-alloy(11$\bar{2}$0)	Cr(001)	MgO(001)	Futamoto et al., 1994 [7]
Co-alloy(11$\bar{2}$0)	Cr(001)	GaAs(001)	Ding et al., 1994 [8]
Co-alloy(1120)	Cr(001)/Ag(001)	Si(001)	Yang et al., 1997 [9]
	Mn_3Si(002)/Ag(001)	Si(001)	Hsu et al., 2000 [10]
Co-alloy(10$\bar{1}$1)	-	Cr(110)	Wong et al., 1991 [4]
Co-alloy(10$\bar{1}$1)	Cr(110) /Ag(111)	Si(111)	Gong et al., 1999 [11]
Co, Co-alloy(10$\bar{1}$0)	Cr(112)	MgO(110), LiF(110)	Nakamura et al., 1994 [5], 1995 [12]
Co-alloy(1010)	Cr(112) /Ag(110)	Si(110)	Yang et al., 1999 [13]
Co, Co-alloy(0001)	Ti(0001), Ru(0001)	Mica(0001)	Krishnan et al., 1994 [14]
Co-alloy(0001)	Ti(0001) /Ag(111)	Si(111)	Gong et al., 1999 [15]
Co-alloy(0001)	CoCrRu(0001)	$SrTiO_3$(111), $LaAlO_3$(0001) Al_2O_3(0001)	Terayama et al., 2001 [16]

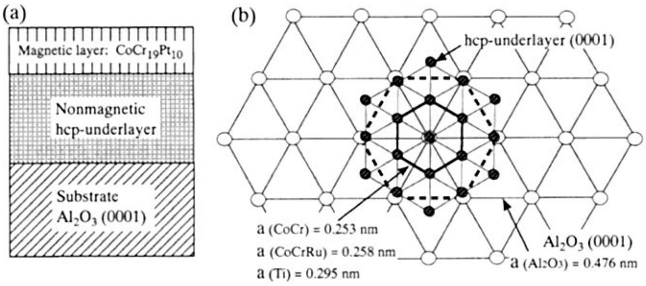

Fig. 1 (a) Cross-sectional view of the sample structure. (b) Crystallographic relationship between the nonmagnetic *hcp*-underlayer and the substrate of Al_2O_3(0001) single crystal. Note that the *a*-axis of the *hcp*-underlayer is rotated by 30 degrees with respect to that of Al_2O_3 substrate.

structure was selected from the group which consists of Ti, $TiCr_{10}$, $CoCr_{40}$, $CoCr_{25}Ru_{25}$, and $CoCr_{25}Ru_{25}$/Ti. The thickness of the $CoCr_{19}Pt_{10}$ magnetic layer was kept constant at 25 nm. The subscripts on the chemical names above are in at% and are the values for the respective sputtering targets.

The rocking curve and pole-figure techniques were employed with X-ray diffraction to investigate the sample structure. Cross-sectional views of the sample structure were obtained through a high-resolution transmission electron microscope. TEM was also used, with a chemical analysis facility, to investigate the microscopic-level distribution of elements in the alloy of a thin film of single-crystal (0001)-oriented $CoCr_{19}Pt_{10}$. A focussed electron beam two nm in diameter was employed in this electron-probe micro-analysis (EPMA) to determine the distribution of elements in the cross-sectional and plan-views of the sample.

3. Results and Discussion

3.1 X-Ray Diffraction

The $\Delta\theta_{50}$ values of (0002) rocking curves measured for the underlayers and the Co-alloy layers are given in Table 2. For the nonmagnetic Co-alloy underlayers, the $\Delta\theta_{50}$ values include the effect of the Co-alloy layers, since the X-ray diffraction peaks for the $CoCr_{40}$ and $CoCr_{25}Ru_{25}$ layers overlapped with those for the magnetic $CoCr_{19}Pt_{10}$ layers. The $\Delta\theta_{50}$ value for the Co-alloy layer is in the range from 0.6 to 3.5 degrees. A $\Delta\theta_{50}$ value below one degree may suggest that the thin film was grown epitaxially on the single-crystal substrate. It is clearly shown that preparation of an epitaxial layer of $CoCr_{19}Pt_{10}$ is strongly dependent on the material used for the underlayer.

Figure 2 shows the X-ray pole-figure profiles measured for the substrates, underlayers, and Co-alloy layers. The {10.1} poles for the nonmagnetic Co-alloy underlayers are overlapped with those for the $CoCr_{19}Pt_{10}$ magnetic layers. The {10.1} pole-figure for the $CoCr_{19}Pt_{10}/Al_2O_3$(0001) sample shows a weak intensity of 6-fold symmetry. This data indicates that the $CoCr_{19}Pt_{10}$ magnetic layer has been grown epitaxially on the Al_2O_3(0001) substrate but with a large texture-induced dispersion. This film presumably includes crystallographic defects such as the subgrain boundaries that were noted in previous studies [14], [15]. The $CoCr_{19}Pt_{10}$ film in the $CoCr_{19}Pt_{10}/TiCr_{10}/Al_2O_3$(0001) sample is polycrystalline, even though the $TiCr_{10}$ underlayer was epitaxially grown on the substrate. The circular distributions of the {10.1} poles for the $CoCr_{19}Pt_{10}$ film in the $CoCr_{19}Pt_{10}/CoCr_{40}/Al_2O_3$(0001) sample, which is formed by circular and arc-like curves, indicate that it, too, is polycrystalline. The {10.1} pole-figures of Co-alloy for the $CoCr_{19}Pt_{10}/CoCr_{25}Ru_{25}/Al_2O_3$(0001) and $CoCr_{19}Pt_{10}/CoCr_{25}Ru_{25}$/Ti/$Al_2O_3$(0001) samples are made up of very sharp reflections in 6-fold symmetry, indicating that the growth of the $CoCr_{19}Pt_{10}$ magnetic layers on the Al_2O_3(0001) substrates was epitaxial.

Of the various underlayers investigated here, the $CoCr_{25}Ru_{25}$ layer produced the sharpest {10.1} pole-figure profile with the smallest dispersion, while the $CoCr_{40}$ layer produced a circular {10.1} pole-figure distribution which had the largest dispersion. The or-

Table 2 $\Delta\theta_{50}$ values for thin films deposited on the $Al_2O_3(0001)$ substrate ($\Delta\theta_{50}$: degs).

Sample structure	Underlayer	Co-alloy layer
(1) CoCrPt (25 nm)	-	3.5
(2) CoCrPt (25 nm)/TiCr (50 nm)	0.6 (TiCr)	3.0
(3) CoCrPt (25 nm)/CoCr (20 nm)	*	2.2 (CoCr + CoCrPt)
(4) CoCrPt (25 nm)/CoCrRu (50 nm)	*	0.6 (CoCrRu + CoCrPt)
(5) CoCrPt (25 nm)/CoCrRu (10 nm)/Ti (50 nm)	0.6 (Ti) *	0.9 (CoCrRu + CoCrPt)

* The X-ray diffraction peak for the nonmagnetic Co-alloy layer overlapped with that for the CoCrPt layer.

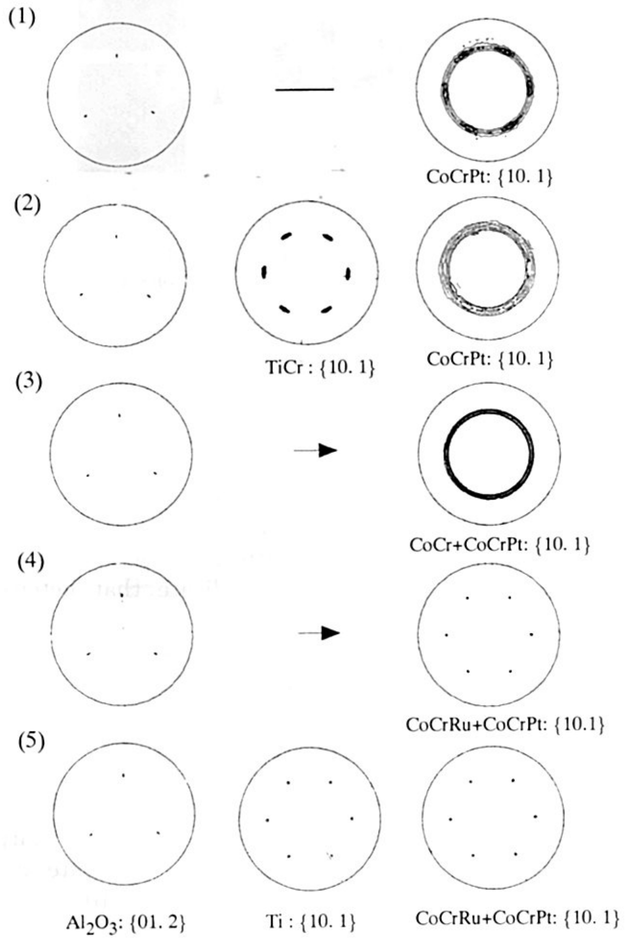

Fig. 2 X-ray pole-figure profiles for 5 samples: (1) $CoCr_{19}Pt_{10}$ (25 nm)/Al_2O_3 (0001), (2) $CoCr_{19}Pt_{10}$ (25 nm)/$TiCr_{10}$(50 nm)/ Al_2O_3(0001), (3) $CoCr_{19}Pt_{10}$ (25 nm)/$CoCr_{40}$ (20 nm)/ Al_2O_3 (0001), (4) $CoCr_{19}Pt_{10}$ (25 nm)/$CoCr_{25}Ru_{25}$ (50 nm)/Al_2O_3 (0001), and (5) $CoCr_{19}Pt_{10}$ (25 nm)/ $CoCr_{25}Ru_{25}$ (10 nm)/Ti (50 nm)/ Al_2O_3(0001).

der of merit for {10.1} pole dispersion of the thin film layers formed on the $Al_2O_3(0001)$ substrates is $CoCr_{25}Ru_{25}(-5.9\%)$ > Ti(7.6%) > $TiCr_{10}(7.3\%)$ > $CoCr_{19}Pt_{10}(-6.6\%)$ > $CoCr_{40}(-6.1\%)$. Here, the numerical values are the degrees of lattice misfit between the deposited material and the $Al_2O_3(0001)$ substrate. The X-ray pole-figure study indicates that the $CoCr_{19}Pt_{10}$ layer has a weak tendency for hetero-epitaxy, while hetero-epitaxy is not realized for the $CoCr_{40}$ layer on the $Al_2O_3(0001)$ substrate. Hetero-epitaxy is realized for the other materials. As the X-ray pole-figure observations clearly show, a small lattice misfit between the deposited layer and the substrate does not always provide a sufficient condition for good hetero-epitaxial growth of thin films.

The $TiCr_{10}$, Ti, $CoCr_{19}Pt_{10}$, and $CoCr_{25}Ru_{25}$ layers grew by epitaxy on the $Al_2O_3(0001)$ substrate. However, the growth of the $CoCr_{40}$ layer was not epitaxial on the $Al_2O_3(0001)$ substrate. The growth of $CoCr_{19}Pt_{10}$ magnetic layer was epitaxial on the $CoCr_{25}Ru_{25}$/Ti(0001) and $CoCr_{25}Ru_{25}(0001)$ layers but not on the $TiCr_{10}(0001)$ layer. It is apparently necessary to take factors other than the lattice misfit into account such as chemical affinity and the diffusion properties of the deposited material on the substrate. An underlayer material which has a large proportion of Cr atoms tends to be a poor base for epitaxial growth on the $Al_2O_3(0001)$ substrate. One possibility is that Cr atoms may suppress the surface diffusion of the material deposited on the substrate through selective combination with the oxygen atoms on the $Al_2O_3(0001)$ surface. Some diffusion of the deposited atoms over the substrate's surface is a necessary precondition for epitaxial growth. The addition of Ru to the CoCr-alloy is considered to facilitate surface diffusion, since the CoCrRu layer showed good hetero-epitaxy on both the $Al_2O_3(0001)$ substrate and the Ti(0001) underlayer. It is interesting to note that hetero-epitaxy between the layers is realized with the Ti(0001) underlayer and $CoCr_{25}Ru_{25}$ layer, even though the misfit between the Ti ($a = 0.295$ nm) and $CoCr_{25}Ru_{25}$ ($a = 0.258$ nm) lattices is a large 12.5%. Surface diffusion of the deposited material over the substrate is considered to play an important role in this formation of an epitaxial thin film of $CoCr_{25}Ru_{25}$ on a Ti(0001) layer. However, further study will be needed to prove this interpretation.

3.2 Transmission Electron Microscopy

In order to investigate the microstructure of the thin films grown by epitaxy on the $Al_2O_3(0001)$ substrates, their cross-sectional structures were observed through a high-resolution TEM. Figure 3 shows the cross-sectional structure and electron diffraction patterns for a $CoCr_{19}Pt_{10}/CoCr_{25}Ru_{25}/Al_2O_3(0001)$ sample. The pattern of electron diffraction from the substrate, Fig. 3(b), is for the $Al_2O_3(1120)$ plane. The electron

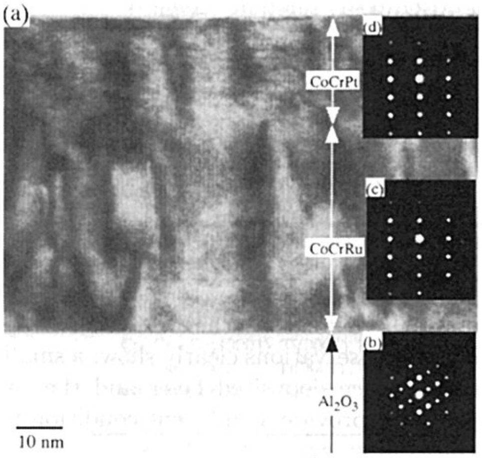

Fig. 3 (a) Cross-sectional view of a $CoCr_{19}Pt_{10}$ (25 nm)/Co $Cr_{25}Ru_{25}$ (50 nm)/Al_2O_3(0001) sample: (b), (c), and (d) show the diffraction patterns for selected areas of the Al_2O_3, $CoCr_{25}Ru_{25}$, and $CoCr_{19}Pt_{10}$ regions, respectively.

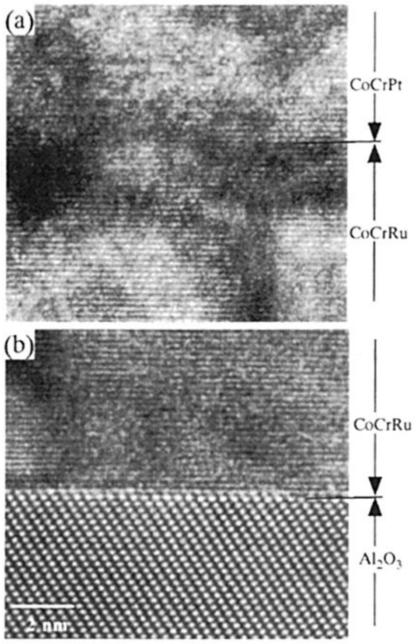

Fig. 4 High-resolution TEM micrographs of a $CoCr_{19}Pt_{10}$ (25 nm)/$CoCr_{25}Ru_{25}$ (50 nm)/ Al_2O_3(0001) sample: (a) the interface between the $CoCr_{19}Pt_{10}$ and $CoCr_{25}Ru_{25}$ layers and (b) the interface between the $CoCr_{25}Ru_{25}$ layer and Al_2O_3(0001) substrate.

diffraction from the $CoCr_{25}Ru_{25}$ layer, Fig. 3(c), and that from the $CoCr_{19}Pt_{10}$ layer, Fig. 3(d), clearly indicate that hetero-epitaxial thin-film growth has been realized on the Al_2O_3(0001) substrate.

Figure 4 is a pair of high-resolution TEM images that show the interfaces between the Al_2O_3(0001) substrate and $CoCr_{25}Ru_{25}$ layer and between the $CoCr_{25}Ru_{25}$ and $CoCr_{19}Pt_{10}$ layers. The good hetero-epitaxy between the Al_2O_3(0001) substrate and the $CoCr_{25}Ru_{25}$ layer is clearly visible. The (0002) planes are parallel for both pairs of materials. Growth of the $CoCr_{19}Pt_{10}$ magnetic layer on the $CoCr_{25}Ru_{25}$ underlayer is perfectly hetero-epitaxial; the lattice misfit is only −0.8%.

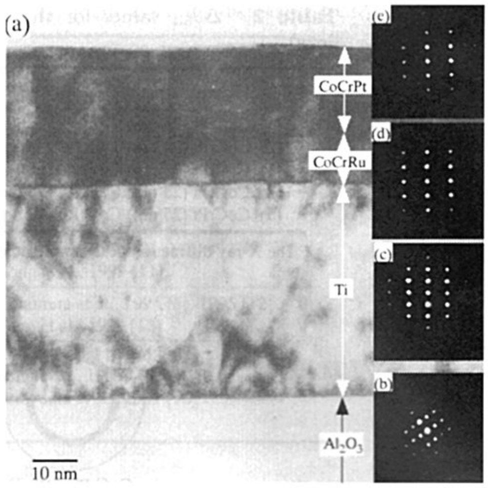

Fig. 5 (a) Cross-sectional view of a $CoCr_{19}Pt_{10}$ (25 nm)/Co $Cr_{25}Ru_{25}$ (10 nm)/Ti (50 nm)/ Al_2O_3(0001) sample: (b), (c), (d), and (e) show the diffraction patterns for selected areas of the Al_2O_3, Ti, $CoCr_{25}Ru_{25}$, and $CoCr_{19}Pt_{10}$ regions, respectively.

Figure 5 shows the cross-sectional structure of a $CoCr_{19}Pt_{10}$/$CoCr_{25}Ru_{25}$/ Ti/Al_2O_3(0001) sample and series of electron diffraction patterns from the respective materials. The patterns indicate that hetero-epitaxial film growth is realized across the different layers. Some dark regions are recognizable in the bright field image for the Ti layer close to both of its boundaries. These are presumably result of stress and/or strain. There are no clear crystalline grain boundaries in either the Ti or the $CoCr_{19}Pt_{10}$/$CoCr_{25}Ru_{25}$ layer.

High-resolution TEM micrographs of the regions around the boundaries are shown in Fig. 6. A sharp boundary is formed between the Al_2O_3 substrate and the Ti underlayer. A noteworthy in Fig. 6(b) is that the Ti(0002) lattice images are not exactly parallel to those of Al_2O_3(0002) layers but are bending with small angles. A similar tendency is visible in the same layer near the $CoCr_{25}Ru_{25}$ layer. There is an atomically disordered region that takes up very few (0002) layers at the interface between the $CoCr_{25}Ru_{25}$ and the Ti layer; that is presumably caused by the large lattice misfit of −12.5% for these materials. The growth of a $CoCr_{25}Ru_{25}$ layer on Ti(0001) is interpreted to be based on a quasi-hetero-epitaxial mechanism where the continuity of the lattice across the boundary is disturbed but the overall crystallographic relationship between the two layers is maintained. This quasi-hetero-epitaxy between Ti and Co-alloy layers may easily be lost by modifying the composition of the thin film as was seen in the case of the $CoCr_{19}Pt_{10}$/$TiCr_{10}$/Al_2O_3(0001) sample in this study. On the other hand, perfect hetero-epitaxy is realized for $CoCr_{19}Pt_{10}$ on $CoCr_{25}Ru_{25}$. This is clearly visible in the upper half of high-resolution lattice image of Fig. 6(a).

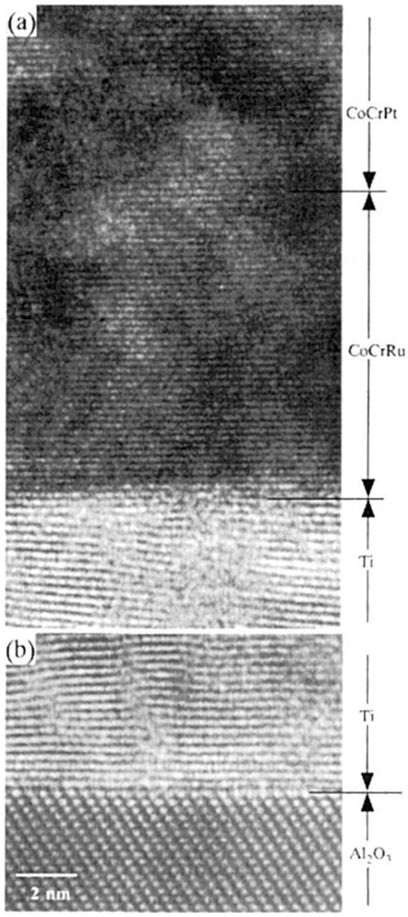

Fig. 6 High-resolution TEM micrographs of a $CoCr_{19}Pt_{10}$ (25 nm)/$CoCr_{25}Ru_{25}$ (10 nm)/Ti (50 nm)/ Al_2O_3(0001) sample: (a) the interfaces of the $CoCr_{19}Pt_{10}$/$CoCr_{25}Ru_{25}$/Ti stack and (b) the interface between the Ti layer and the Al_2O_3(0001) substrate.

3.3 Chemical Compositions

Local composition was investigated by applying an EPMA-TEM technique to a cross-section through a sample of $CoCr_{19}Pt_{10}/CoCr_{25}Ru_{25}/Al_2O_3$(0001). Compositional variations of the alloy elements of Co, Cr, Pt, and Ru were investigated along the sequences of points on two lines shown in Fig. 7(a). Similar proportions for the respective elements were observed along both lines. There are no large differences in elements in composition along the film growth direction in either the $CoCr_{25}Ru_{25}$ or the $CoCr_{19}Pt_{10}$ layer. Compositional fluctuations along the direction of film growth are less than 3 at.% for each of the elements in the alloys. Sharp compositional variations of a very few nanometers appear at the interface between the $CoCr_{25}Ru_{25}$ and $CoCr_{19}Pt_{10}$ layers. When we consider the electron-probe's diameter 2 nm and the uncertainty in terms of sample thickness, we see that it is not easy to determine an accurate diffusion distance for elements when this value is a very small number of nanometers.

Figure 8 shows local concentrations of Co, Cr, and Pt for a plan-view thin film of single-crystal $CoCr_{19}Pt_{10}$(0001) which was extracted from a $CoCrPt/CoCrRu/Al_2O_3$(0001) sample. The compositional analysis was carried out along the two lines, A–B and C–D, indicated in Fig. 8(c). The film's composition was determined as Co 71.2 $\pm$ 2.8(2σ)%, Cr 18.0 $\pm$ 2.3(2σ)%, and Pt 10.8 $\pm$ 1.1(2σ)%, where σ is the standard deviation. This thin film thus shows slight compositional variation, though it is a (0001)-oriented single-crystal. Such compositional fluctuations may be due to the effect of local stress or strain within the single-crystal thin film sample. Compositional fluctuations will readily be enhanced by the presence of crystallographic defects in a CoCr-alloy sample where the proportion of Cr exceeds the limit on solubility in the phase diagram for the Co-Cr alloy system.

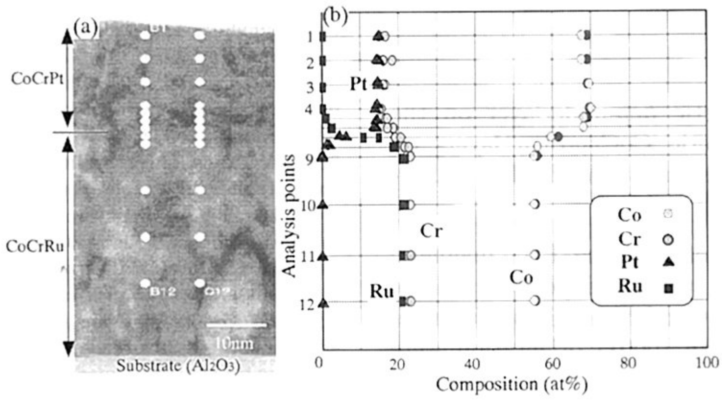

Fig. 7 Distributions of Co, Cr, Pt, and Ru in the alloys, as measured along the direction of thin film growth: (a) a cross-sectional TEM micrograph of $CoCr_{19}Pt_{10}$ (25 nm)/$CoCr_{25}Ru_{25}$ (50 nm)/ Al_2O_3(0001) sample: white dots indicate the analysis points, and (b) distribution of the alloy elements.

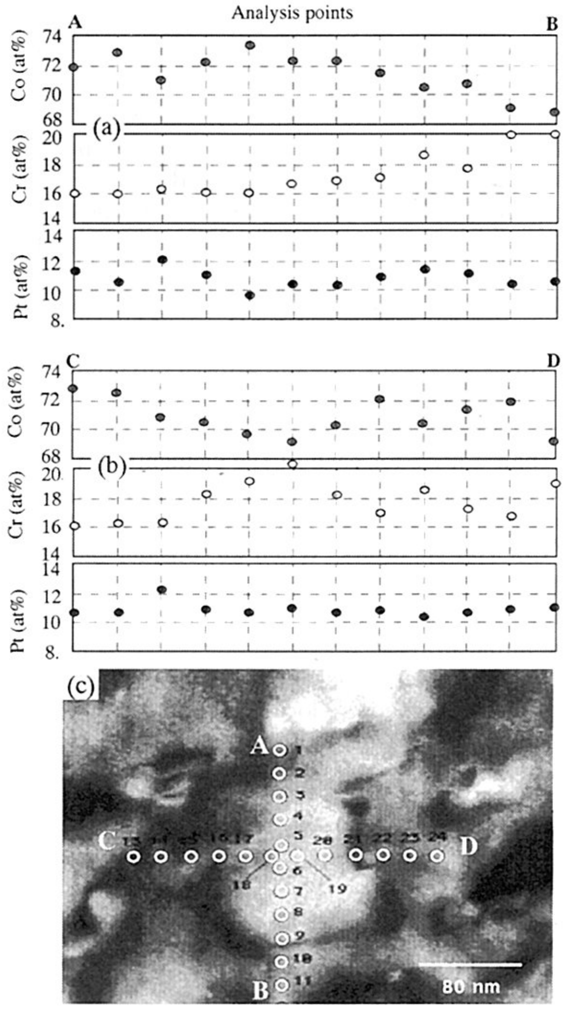

Fig. 8 Distributions of Co, Cr, and Pt measured for a thin film of $CoCr_{19}Pt_{10}$ single-crystal; the $CoCr_{19}Pt_{10}$ plan-view specimen was extracted from a $CoCr_{19}Pt_{10}$ (25 nm)/$CoCr_{25}Ru_{25}$ (50 nm)/Al_2O_3(0001) sample: (a) distributions of elements as measured along the A–B line, (b) distributions of elements as measured along the C–D line, and (c) a plan-view TEM image showing the analysis points.

4. Conclusions

The effect of a nonmagnetic *hcp*-underlayer on the epitaxial growth of magnetic $CoCr_{19}Pt_{10}$ layers on Al_2O_3(0001) substrates was investigated. The following results were obtained.

(1) The epitaxial growth of a $CoCr_{19}Pt_{10}$ magnetic layer was found to be strongly dependent on the underlayer material. Good thin films of single-crystal $CoCr_{19}Pt_{10}$ with (0001) orientation were obtained by deposition on Al_2O_3(0001) substrates via $CoCr_{25}Ru_{25}$ or $CoCr_{25}Ru_{25}$/Ti underlayers. A weak form of hetero-epitaxy was realized when the $CoCr_{19}Pt_{10}$ film was directly deposited on the substrate, while polycrystalline thin films grew when either a $TiCr_{10}$ or a $CoCr_{40}$ underlayer was employed.

(2) The growth of $CoCr_{19}Pt_{10}$ film on Ti(0001) is according to a quasi-hetero-epitaxial mechanism where the continuity of the lattice across the boundary is disturbed but the overall crystallographic relationship between the two layers is maintained.

(3) Epitaxially grown thin films $CoCr_{19}Pt_{10}$ have compositional variations across the film plane of a few percent in terms of the concentrations of elements.

Acknowledgment

A part of this work was carried out under the ASET program supported by NEDO.

References

[1] N. Inaba, T. Yamamoto, Y. Hosoe, and M. Futamoto, "Microstructural segregation in CoCrTa and CoCrPt longitudinal magnetic recording media," J. Magn. Magn. Mater., vol.168, pp.222–231, 1997.

[2] N. Inaba, Y. Uesaka, and M. Futamoto, "Compositional and temperature dependence of basic magnetic properties of CoCr-alloy thin films," IEEE Trans. Magn., vol.36, no.1, pp.54–60, 2000.

[3] J. Daval and D. Randet, "Electron microscopy on high-coercive-force Co-Cr composite films," IEEE Trans. Magn., vol.MAG-6, no.4, pp.768–773, 1970.

[4] B.Y. Wong, D.E. Laughlin, and D.N. Lambeth, "Investigation of CoNiCr thin films deposited on [100] and [110] Cr single crystals," IEEE Trans. Magn., vol.27, no.6, pp.4733–4735, 1991.

[5] A. Nakamura and M. Futamoto, "Epitaxial growth of Co/Cr bilayer films on MgO single crystal substrates," Jpn. J. Appl. Phys., vol.32, pp.L1410–L1413, 1993.

[6] A. Nakamura and M. Futamoto, "Epitaxial growth and microstructures of Co/Cr bilayer films deposited on single crystal substrates," Trans. Mat. Res. Soc. Jpn., vol.15B, pp.787–790, 1994.

[7] M. Futamoto, M. Suzuki, N. Inaba, A. Nakamura, and Y. Honda, "Magnetic and recording characteristics of bicrystalline longitudinal recording medium formed on an MgO single crystal disk substrate," IEEE Trans. Magn., vol.30, no.6, pp.3975–3977, 1994.

[8] J. Ding and J.-G. Zhu, "Microstructure and recording properties of bicrystal disks with GaAs substrates," IEEE Trans. Magn., vol.30, no.6, pp.3978–3980, 1994.

[9] W. Yang, D.N. Lambeth, L. Tang, and D.E. Laughlin, "Epitaxial Ag templates on Si(001) for bicrystal CoCrTa media," J. Appl. Phys., vol.81, pp.4370–4372, 1997.

[10] Y.-N. Hsu, D.E. Laughlin, and D.N. Lambeth, "Growth of CoCrTa(1120)-oriented thin films on DO_3-Mn_3Si(002) underlayer," J. Appl. Phys., vol.87, pp.6698–6700, 2000.

[11] H. Gong, W. Yang, M. Rao, D.E. Laughlin, and D.N. Lambeth, "Epitaxial growth of quad-crystal Co-alloy magnetic recording media," IEEE Trans. Magn., vol.35, no.5, pp.2676–2678, 1999.

[12] A. Nakamura, M. Koguchi, and M. Futamoto, "Microstructure of Co/Cr bilayer films epitaxially grown on MgO single-crystal substrates," Jpn. J. Appl. Phys., vol.34, pp.2307–2311, 1995.

[13] W. Yang, D.N. Lambeth, and D.E. Laughlin, "Single crystal Co-alloy media on Si(110)," J. Appl. Phys., vol.85, pp.4723–4725, 1999.
[14] K.M. Krishnan, T. Takeuchi, Y. Hirayama, and M. Futamoto, "Epitaxial growth and enhanced saturation megnetization of single crystal $Co_{1-x}Cr_x$ media suitable for perpendicular magnetic recording," IEEE Trans. Magn., vol.30, no.6, pp.5115–5119, 1994.
[15] H. Gong, M. Rao, D.E. Laughlin, and D.N. Lambeth, "Highly oriented perpendicular Co-alloy media on Si(111) substrates," J. Appl. Phys., vol.85, no.8, pp.4699–4701, 1999.
[16] K. Terayama, K. Sato, Y. Hirayama, N. Inaba, and M. Futamoto, "Preparation of C-axis oriented CoCrPt single-crystal thin films on oxide single-crystal substrates," J. Mag. Soc. Jpn., vol.25, pp.559–562, 2001.
[17] Y. Matsuda, M. Suzuki, Y. Hirayama, Y. Honda, and M. Futamoto, "Co-Cr-Ta/Ti/TiCr perpendicular recording disks prepared using an UHV sputtering system," J. Mag. Soc. Jpn., vol.18, Suppl. no.S1, pp.99–102, 1994.
[18] K. Ouchi, "Review on recent developments of perpendicular recording media," IEICE Trans. Electron., vol.E84-C, no.9, pp.1121–1131, Sept. 2001.
[19] Y. Hirayama, M. Futamoto, K. Ito, Y. Honda, and Y. Maruyama, "Development of high resolution and low noise single-layer perpendicular recording media for high density recording," IEEE Trans. Magn., vol.33, no.1, pp.996–1001, 1997.
[20] M. Futamoto, Y. Hirayama, Y. Honda, A. Kikukawa, K. Tanahashi, and A. Ishikawa, "CoCr-alloy perpendicular magnetic recording media for high-density recording," J. Mag. Mag. Mater., vol.235, pp.281–288, 2001.

Masaaki Futamoto received the B.E., M.E., and Dr. degrees in materials science from Osaka University in 1971, 1973, and 1982, respectively. He joined Central Research Laboratory (CRL), Hitachi Ltd., in 1973 and worked on electron emissive materials. From 1982 to 1983, he was a visiting scientist at the University of Sussex, U.K. Since 1983, he has been engaged in the research and development of magnetic thin films for high-density magnetic recording. He is currently chief research scientist in CRL, Hitachi Ltd. He has served as a leader of media research group in a Japanese national project (ASET) that was established to develop future oriented magnetic recording technologies from 1996 to 2001. He was a visiting professor at Tokyo University of Agriculture and Technology for the period between 1999 and 2001. He is serving as the chairman of the Technical Committee of Magnetic Recording of IEICE. He is also a member of the Institute of Image Information and Television Engineers, the Magnetics Society of Japan, the Japan Institute of Metals, the Surface Science Society of Japan, the Applied Physical Society of Japan, the Materials Research Society (MRS), and is qualified as a Fellow of the IEEE since 2002.

Kouta Terayama received the B.E. and M.E. degrees from Tokyo University of Agriculture and Technology in 1999 and 2001. He is currently with the Canon Inc.

Katsuaki Sato received the B.S., and M.S. degrees in electrical engineering from Kyoto University in 1964, and 1966, respectively. In 1966 he was employed by NHK (Japan Broadcasting Corporation). After two years training at Osaka Broadcasting Station, he joined in 1968 the Broadcasting Research Laboratory of NHK as a researcher in magnetic materials. He worked on magnetic semiconductors, magneto-optical spectroscopy and magneto-optical disk technology. He submitted a doctoral thesis to Kyoto University for which he was given a doctor of Engineering in 1978. In 1984 he was appointed as an Associate Professor of Faculty of Technology, Tokyo University of Agriculture and Technology. His works have been in the fields of magnetic semiconductors, magneto-optical effect, magneto-optical recording techniques, nano-fabrication and nano-observation of magnetic superstructures. Professor Sato received the Publication Award to the book "Hikari to Jiki (Light and Magnetism)" in 1997, the Paper Award in 2001, both from the Magnetics Society of Japan.

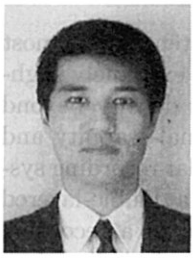

Yoshiyuki Hirayama received the B.E. and M.E. from Kyoto University in 1986 and 1988, respectively. He joined CRL, Hitachi Ltd. in 1988 and worked on magnetic thin films for high-density magnetic recording. Mr. Hirayama is a member of the Magnetics Society of Japan.